Frontiers of Physics
https://doi.org/10.1007/s11467-019-0938-8
Front. Phys.
14(6), 62601 (2019)

RESEARCH ARTICLE

Photonic spin Hall effect in PT symmetric metamaterials

Yang-Yang Fu[*,†], **Yue Fei**[*], **Da-Xing Dong**, **You-Wen Liu**[‡]

College of Science, Nanjing University of Aeronautics and Astronautics, Nanjing 211106, China
Corresponding authors. E-mail: †yyfu@nuaa.edu.cn, ‡ywliu@nuaa.edu.cn
Received October 9, 2019; accepted October 21, 2019

We proposed and demonstrated that PT symmetric metamaterials could be used to achieve enhanced spin Hall effect (SHE) of light. We find that when laser mode is excited in PT symmetric system, the enhanced SHE could be obtained in both transmitted and reflected beams. In addition, as exceptional points (EPs) of PT symmetric system can happen for both p- and s-polarizations, the enhanced SHE of reflected light can function for both horizontally and vertically polarized incident beams. Particularly, these EPs can lead to unidirectional reflectionlessness, asymmetric SHE with maximum contrast ratio of 48 is obtained by launching light beams near EPs. Our work opens up a new path to obtain enhanced transverse displacement for both reflected and transmitted light and enables more opportunities in manipulating photonic SHE.

Keywords PT symmetry, exceptional points, laser mode, spin Hall effect

1 Introduction

As the counterpart of spin Hall effect (SHE) in electronic systems, photonic SHE [1, 2] refers to the splitting of opposite spin photons (the right and left circular polarizations of light beam) perpendicular to the incident plane. The SHE of light has been widely investigated in many physical systems, such as glass [3], dielectric-meal barrier [4], and polymeric material [5], etc. In general, due to weak light-matter interaction, the spin-dependent splitting is limited to a fraction of one wavelength [6], which hinders the potential applications. It was experimentally found that by launching incident beam near the Brewster angle [7–9], the SHE of reflected light could be enhanced, yet limited in horizontally polarized incident beam. However, this method is not available to obtain enhanced SHE of transmitted light.

In the past years, metamaterials [10], artificially engineered subwavelength structures, have enabled people to control wave in an innovative way and therefore provide a new route to exploring photonic SHE. A variety of metamaterials have been employed to investigate photonic SHE, such as hyperbolic metamaterials [11, 12], chiral metamaterials [13], metasurfaces (2D metamaterials) [14]. In particular, zero index metamaterials (ZIMs), featured with near-zero refractive index, have exhibited their special abilities in wave manipulation, such as unidirectional transmission [15] and cavity mode resonance [16, 17]. Much effort has devoted to the investigation on the enhanced SHE of transmitted light in ZIMs [18–21]. Generally, intrinsical loss in metamaterials can greatly destroy the performance of efficient devices, however SHE of transmitted light could be enhanced by introducing losses in anisotropic ZIMs [19, 20]. Alternatively, one of the approaches to relieve the drawback of loss is adding optical gain portion into metamaterials, particularly for the metamaterials with balanced loss and gain, which enables new physical phenomena. Recent advance in non-Hermitian optics has shown that a large number of novel phenomena could be realized in parity–time (PT) symmetric systems [22], where PT symmetric configuration is realized by spatially modulating balanced gain and loss, i.e., $n(x) = n^*(-x)$. For example, unidirectional reflectionless light propagation can be achieved at exceptional points (EPs) [23, 24], and coherent perfect absorber (CPA) and laser modes can coexist in a single structure [25, 26]. Therefore, PT symmetric metamaterials, as new material platforms, could be potentially used to explore enhanced photonic SHE. Meanwhile, new effects of photonic SHE in PT symmetric structures still remains unrevealed.

In this work, we employ PT symmetric metamaterials to study photonic SHE and reveal unknown effect of spin-dependent splitting. We find that when laser mode is excited in a simple structure of PT symmetric bilayer, which leads to intensive transmission and reflection, the transverse displacement of spin-dependent splitting could be enhanced in both reflected and transmitted light, with the maximum transverse displacement of nearly 4.3λ. In addition, the transverse displacement of reflected light could be enhanced by launching incident beams near EPs staying away from the laser mode; while for EPs close to the laser mode, the enhanced transverse displacement of reflected light via EPs is suppressed due to the intense resonance of the laser mode. More interestingly, as EPs can induce unidirectional reflectionless light propagation,

*Y. Fu and Y. Fei contributed equally to this work.

© Higher Education Press and Springer-Verlag GmbH Germany, part of Springer Nature 2019

asymmetric SHE of reflected light could be realized near EPs away from the laser mode. To be exact, for a particular incidence near EPs, large spin splitting of reflected light happens for the incidence from one side and tiny spin splitting occurs for the incidence from the other side, and the maximum contrast ratio of the asymmetric transverse displacements is approximatively 48. Therefore, our work provides an effective way to manipulate photonic SHE, and also may facilitate more exploration of photonic SHE in non-Hermitian systems.

2 Theory and model

Now we consider an incident beam with Gaussian distribution, and its angular spectrum can be written as $\tilde{E}_i = w_0 \exp[-w_0^2(k_{ix}^2 + k_{iy}^2)/4]/\sqrt{2\pi}$ (w_0 is the beam waist). As shown in Fig. 1, the incident plane is located in the x–z plane and the transverse displacement is along the y-axis. Hence, the angular spectra between reflected and incident light beams is written as

$$\begin{pmatrix} \tilde{E}_r^H \\ \tilde{E}_r^V \end{pmatrix} = \begin{pmatrix} r_p & \dfrac{k_{ry}(r_p + r_s)\cot\theta_i}{k_0} \\ -\dfrac{k_{ry}(r_p + r_s)\cot\theta_i}{k_0} & r_s \end{pmatrix} \begin{pmatrix} \tilde{E}_i^H \\ \tilde{E}_i^V \end{pmatrix}, \tag{1}$$

where $\tilde{E}_{r(i)}^H$ and $\tilde{E}_{r(i)}^V$ denote the horizontal (H) and vertical (V) components of angular spectra of reflected (incident) beam components, r_p and r_s denote the Fresnel reflection coefficients for p-polarization and s-polarization, respectively, $k_0 = 2\pi/\lambda$ is wave vector in air, θ_i is the incident angle, $k_{ry} = k_{iy}$ and $k_{rx} = -k_{ix}$ due to momentum conservation at the boundary. Horizontal and vertical polarizations, i.e., the synonym of p-polarization and s-polarization, respectively, mean polarization in the incident plane. At a given plane $z = \text{const}$, the transverse displacement of reflected field is defined as

$$\delta_\pm = \frac{\iint y_r I_\pm(x_r, y_r, z_r)\mathrm{d}x_r\mathrm{d}y_r}{\iint I_\pm(x_r, y_r, z_r)\mathrm{d}x_r\mathrm{d}y_r}, \tag{2}$$

and by considering in-plane and out-plane spreads of wave vectors, the analytical expressions of spin-dependent splitting of reflected light can be written as [9]

$$\begin{cases} \delta_\pm^H = \pm C w_0 \dfrac{|r_p|^2 + \mathrm{Re}[r_p r_s^*]}{|r_p|^2 C^2 + |r_p + r_s|^2 + \left|\frac{\partial r_p}{\partial \theta_i}\right|^2 \tan^2\theta_i}, \\ \delta_\pm^V = \pm C w_0 \dfrac{|r_s|^2 + \mathrm{Re}[r_s r_p^*]}{|r_s|^2 C^2 + |r_p + r_s|^2 + \left|\frac{\partial r_s}{\partial \theta_i}\right|^2 \tan^2\theta_i}, \end{cases} \tag{3}$$

where $C = k_0 w_0 \tan\theta$. Similarly, the analytical expressions of spin-dependent splitting of transmitted light is expressed as [11]

$$\begin{cases} \delta_\pm^H = \pm C w_0 \dfrac{|t_p|^2 - \mathrm{Re}[t_p t_s^*]}{|t_p|^2 C^2 + |t_p - t_s|^2 + \left|\frac{\partial t_p}{\partial \theta_i}\right|^2 \tan^2\theta_i}, \\ \delta_\pm^V = \pm C w_0 \dfrac{|t_s|^2 - \mathrm{Re}[t_s t_p^*]}{|t_s|^2 C^2 + |t_p - t_s|^2 + \left|\frac{\partial t_s}{\partial \theta_i}\right|^2 \tan^2\theta_i}. \end{cases} \tag{4}$$

In addition, when $(k_0 w_0)^2 \gg \cot^2\theta_i$ and by neglecting the derivative terms, Eq. (3) and Eq. (4) will be further simplified as

$$\begin{cases} \delta_\pm^H = \pm \dfrac{1 + (|r_s|/|r_p|)\cos(\varphi_s - \varphi_p)}{k_0 \tan\theta_i}, \\ \delta_\pm^V = \pm \dfrac{1 + (|r_p|/|r_s|)\cos(\varphi_s - \varphi_p)}{k_0 \tan\theta_i}, \end{cases} \tag{5}$$

for the reflected light beam [27], where $r_{p(s)} = |r_{p(s)}|\exp(\mathrm{i}\varphi_{p(s)})$,

$$\begin{cases} \delta_\pm^H = \pm \dfrac{1 - (|t_s|/|t_p|)\cos(\varphi_s - \varphi_p)}{k_0 \tan\theta_i}, \\ \delta_\pm^V = \pm \dfrac{1 - (|t_p|/|t_s|)\cos(\varphi_s - \varphi_p)}{k_0 \tan\theta_i}, \end{cases} \tag{6}$$

for the transmitted light beam [4], where $t_{p(s)} = |t_{p(s)}|\exp(\mathrm{i}\varphi_{p(s)})$, which are more straightforward to observe the enhanced SHE of light.

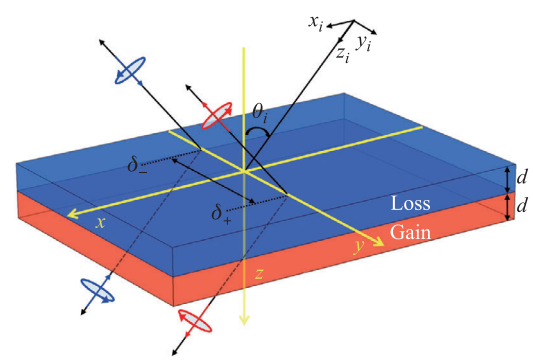

Fig. 1 Illustration of photonic SHE through a PT symmetric bilayer. When the PT symmetric bilayer is illuminated by a linearly polarized beam, it will split into right-handed (red circle) and left-handed (blue circle) circularly polarized components, leading to transverse displacements δ_+ and δ_- ($\delta_+ = \delta_-$), respectively, in both reflected and transmitted beams.

3 Wave scattering in PT symmetric bilayer

Based on the simplified formulas for spin-dependent splitting in Eq. (5) and Eq. (6), we can see the transverse displacements of photonic SHE are highly depending on the transmission/reflection amplitudes of both linear polarized beams, i.e., p-polarized light and s-polarized light, which are crucial elements to achieve enhanced photonic SHE. Different from common media, PT symmetric systems can exhibit some extraordinary phenomena, e.g., unidirectional reflectionlessness and CPA-laser modes, which potentially enable new effects of photonic SHE, such as enhanced SHE of transmitted and reflected light and asymmetric SHE of reflected light. In this study, we consider a simple structure of PT symmetric bilayer [28] to reveal some new effects of photonic SHE. Similar results are also available in other PT symmetric systems. The proposed structure is shown in Fig. 1, in which a pair of slabs with PT symmetry are immersed in air and the loss and gain layers share an identical thickness of d. The relative permittivities of the PT symmetric layers are $\varepsilon_L = \varepsilon_1 + \mathrm{i}\varepsilon_2$ (loss) and $\varepsilon_G = \varepsilon_1 - \mathrm{i}\varepsilon_2$ (gain), and their permeabilities are $\mu = 1$. For the light beam with θ_i incident from the loss side or gain side, the corresponding reflection and transmission coefficients could be obtained using transfer matrix. The transfer matrix for the optical modulation from $z = 0$ to $z = 2d$ can be written as

$$\begin{pmatrix} A_i(z) \\ B_i(z) \end{pmatrix} = \begin{pmatrix} M_{11} & M_{12} \\ M_{21} & M_{22} \end{pmatrix} \begin{pmatrix} A_i(0) \\ B_i(0) \end{pmatrix}, \tag{7}$$

where A_i (B_i) notes for the amplification of light propagating forward (back forward). The reflection and transmission coefficients can be expressed in terms of the matrix elements of M [23], i.e.,

$$t_L = t_G = t = \frac{1}{M_{22}}, \quad r_L = -\frac{M_{21}}{M_{22}}, \quad r_G = \frac{M_{12}}{M_{22}}, \tag{8}$$

where t_L and t_G (r_L and r_G) are the transmission (reflection) coefficients for incident waves from the loss and gain sides, respectively. To conveniently reveal the underlying PT symmetric behaviors, the eigenvalues of scattering matrix ($S = \left(\begin{smallmatrix} t & r_L \\ r_G & t \end{smallmatrix}\right)$) is employed [29, 30], given as $S_\pm = t \pm \sqrt{r_L r_G}$. In order to access more extraordinary phenomena and make a comparison of SHE between PT symmetric metamaterials and ZIMs, the PT symmetric system is optimized as $\varepsilon_1 = \varepsilon_2 = 0.1$ and $d = 0.785\lambda$. The corresponding absolute values of the eigenvalues for p-polarized light are displayed in Fig. 2(a), where there are four special positions in the angular spectrum marked by black arrows to achieve extraordinary phenomena, which are labelled as EP_1, EP_2, EP_3, and CPA-laser mode, respectively. Three incident angles indicated by the solid arrows are EPs, which correspond to unidirectional reflectionlessness and one incident angle marked by the dashed arrow is CPA-laser mode, which could induce quite intense transmission and reflection independent of incident directions [29]. We also show the corresponding relationship between transmission/reflection and incident angle for p-polarized light in Fig. 2(b), where unidirectional reflectionlessness is seen at $\theta_1 = 8.67°$ and $\theta_3 = 23.12°$ for the incidence from the loss side and $\theta_2 = 19.66°$ for the incidence from the gain side, and laser mode is achieved at $\theta_{las} = 21.87°$. While for the case of s-polarized light, only one EP (marked as EP_4) appears at the angular spectrum [see Fig. 2(c)], and unidirectional reflectionlessness appears at $\theta_4 = 7.01°$ for the incidence from the loss side [see Fig. 2(d)]. In the following, we will use these polarization-dependent extraordinary phenomena in the PT symmetric system to explore the SHE for both transmitted and reflected light. As these extraordinary phenomena are limited in $\theta_i \in [0°, 40°]$, we will also explore the SHE in this incident range.

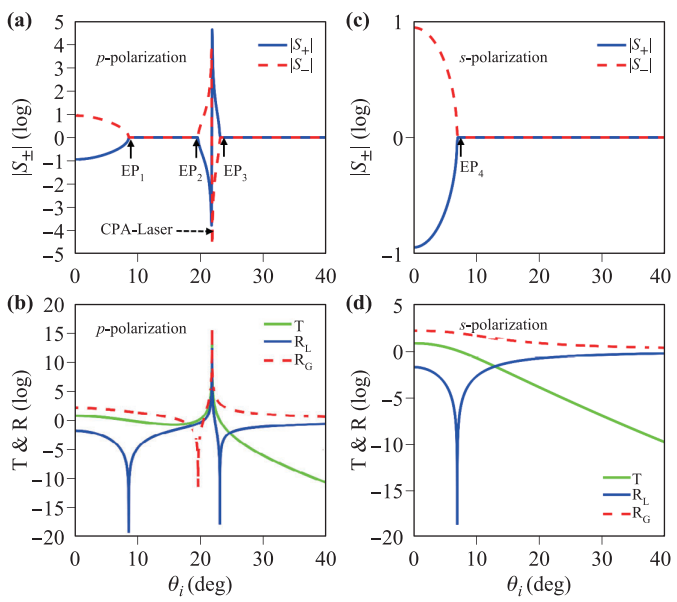

Fig. 2 Wave scattering in PT symmetric bilayer. **(a)** and **(b)** are the absolute values of the eigenvalues of the S-matrix and transmission/reflection in a logarithm scale for p-polarized light, respectively. **(c)** and **(d)** are the corresponding results for s-polarized light. In calculation, we have $\varepsilon_1 = \varepsilon_2 = 0.1$ and $d = 0.785\lambda$ for the PT symmetric metamaterials.

4 Spin Hall effect of transmitted and reflected light

Let us start from the SHE of transmitted light in the PT symmetric bilayer. We show the spectrum of transmission for both s- and p-polarizations with a logarithm scale in Fig. 3(a), where there is an intensive transmission for p-polarization induced by the laser mode. Normally,

the SHE of transmitted light in common media is weak, while for the media with near-zero refractive index, the transverse displacements could be improved around the near-zero Brewster angle [18]. To make a comparison of SHE between an epsilon-near-zero (ENZ) slab and the PT symmetric bilayer, the corresponding spectrum of transmission for the lossless ENZ ($\varepsilon = 0.1$ and $\mu = 1$) slab with $t = 2d = 1.57\lambda$ is shown in Fig. 3(a), where unity transmission for p-polarization is observed at its Brewster angle. As the ratio of $|t_s|/|t_p|$ is a small value in these two systems, the transverse displacements of H-polarized incident light should be tiny for both cases, which can be deduced from the simplified formula in Eq. (6). We use the general formula in Eq. (4) to calculate the transverse displacement of H-polarized incident light shown in Fig. 3(b), where the green solid and black dashed curves denote the cases of the PT symmetric bilayer and the lossless ENZ, respectively. We can see that the transverse displacements from both cases are comparable, implying that the intensive transmission from the laser mode of p-polarization does not have deep influence on the transverse displacement of δ^H, only introducing a dip in the transverse displacement. As the intensive resonance of laser mode can lead to infinite value of $|\partial t_p/\partial\theta_i|^2 \tan^2\theta_i$ [see Fig. 3(c)], such a derivative term is dominant in the denominator of Eq. (4), bringing about a vanishing δ^H at the resonant angle of laser mode. For the transverse displacement of δ^V, when the laser mode of p-polarization is excited, the ratio of $|t_p|/|t_s|$ in the PT symmetric bilayer goes to an infinite value, while the derivative term $|\partial t_s/\partial\theta_i|^2 \tan^2\theta_i$ is tiny [see Fig. 3(c)]. As a result, the enhanced transverse displacement of δ^V appears near the resonant angle of laser mode ($\delta^V \approx 1/|t_p| \cong 0$ at the laser mode), which is indicated by the green solid curve in Fig. 3(d), and the maximum value of the transverse displacement is about 4.3λ, which is larger than that in the lossless ENZ case near its Brewster angle. In addition, the sign change of the enhanced transverse displacement of transmitted light cross the laser mode is observed, which is caused by the phase change of π at the laser mode [29]. Based on the results shown in Fig. 3, we can conclude that the transverse displacement of transmitted light could be greatly enhanced by exciting laser mode in PT symmetric systems, which provides an alternative way to achieve enhanced SHE of transmitted light.

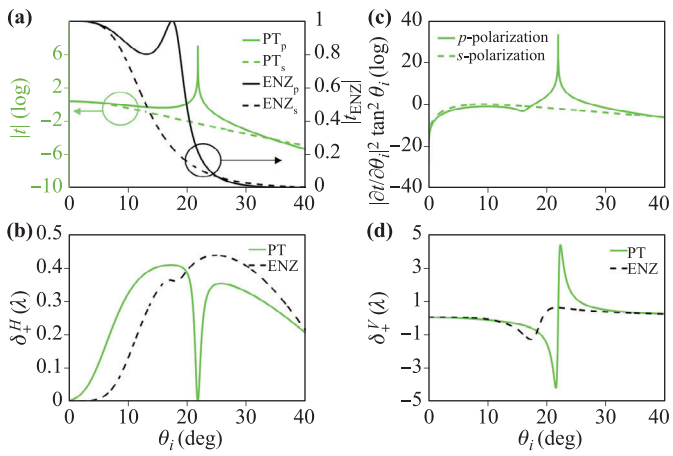

Fig. 3 Photonic SHE of transmitted light in the PT symmetric bilayer. **(a)** The transmission of PT bilayer (left column) and ENZ slab (right column). The transverse displacements of δ_+^H **(b)** and δ_+^V **(d)** of transmitted light, where the solid and dashed curves denote the cases of PT bilayer and ENZ slab. **(c)** The derivative terms $|\partial t/\partial\theta_i|^2 \tan^2\theta_i$ of the $p(s)$-polarization for PT symmetric bilayer, where the solid (dashed) curves denote the cases of $p(s)$ polarization, respectively. In calculation, $w_0 = 15\lambda$.

Here we will investigate the photonic SHE of reflected light in the PT symmetric bilayer and the corresponding results are displayed in Fig. 4, in which the upper (lower) plots described by the blue (red) curves are the relevant results for the reflection from the loss (gain) side and the black curves are the corresponding results of the ENZ slab. For the reflection from the loss side, two EPs (EP_1, EP_3) of p-polarization are seen in Fig. 4(a). Following the simplified formula in Eq. (5), the enhanced transverse displacement of δ^H should be realized by the large ratio of $|r_s|/|r_p|$. By using the general formula in Eq. (3), the corresponding transverse displacement of δ^H is revealed in Fig. 4(b), in which the result of the ENZ slab is shown by the black dashed curve. As seen in Fig. 4(b), the enhanced transverse displacements near EPs (solid curves) exhibit similar results with that from the ENZ medium near its Brewster angle. But surprisingly, the enhanced transverse displacement is only found near EP_1 and the transverse displacement near EP_3 is suppressed. It is because that the resonant angle of EP_1 is far away from that of the laser mode, the derivative term $|\partial r_{L(p)}/\partial\theta_i|^2 \tan^2\theta_i$ is a tiny value; while the resonant angle of EP_3 is close to that of the laser mode, a large value of the derivative term is achieved, which suppresses the enhanced SHE [see Eq. (4)]. These results are well revealed in Fig. 4(c), where EP_3 ($\theta_3 = 23.12°$) locates near the laser mode ($\theta_{las} = 21.87°$) and the derivative term is a large value. Therefore, the expectantly enhanced SHE near EP_3 is suppressed by the excited laser mode. For the SHE in V-polarized beam, apparently, the reflection of s-polarization from the loss side [see Fig. 4(a)] encounters only one EP_4 without laser mode. As a result, the enhanced transverse displacement of δ^V is achieved around EP_4, as shown in Fig. 4(d). In addition, the large ratio of $|r_p|/|r_s|$ is obtained through the laser mode from p-polarization and the derivative term of $|\partial r_{L(s)}/\partial\theta_i|^2 \tan^2\theta_i$ is tiny [see Fig. 4(c)]. Accordingly, the enhanced transverse displacement of δ^V is realized near the laser mode ($\delta^V \approx 1/|r_{L(p)}| \cong 0$ at the laser mode), with a maximum value of about 4.4λ [see Fig. 4(d)]. While for the reflection from the gain side, the extraordinary phenomena are EP_2 and the laser mode from p-polarization [see Fig. 4(e)], which could bring en-

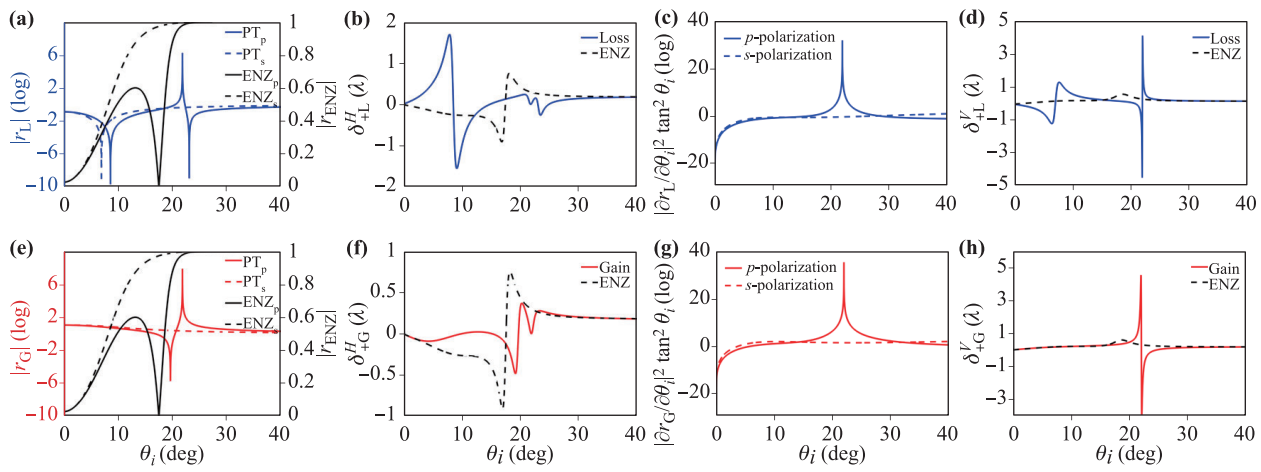

Fig. 4 Photonic SHE of reflected light in the PT symmetric bilayer. The reflection of PT bilayer (left column) and ENZ slab (right column) for the incidence from loss **(a)** and gain **(e)** sides. The transverse displacement of δ^H for the incidence from loss **(b)** and **(f)** gain sides, where the solid and dashed curves denote the cases of PT bilayer and ENZ slab. The derivative terms $|\partial r/\partial\theta_i|^2\tan^2\theta_i$ of the $p(s)$-polarization for the incidence from the loss **(c)** and gain **(g)** sides, where the solid (dashed) curves denote the cases of $p(s)$-polarization, respectively. The transverse displacements of δ^V for the incidence from loss **(d)** and **(h)** gain sides, where the solid and dashed curves denote the cases of PT bilayer and ENZ slab. In calculation, $w_0 = 15\lambda$.

hanced transverse displacement of δ^H and enhanced transverse displacements of δ^V, respectively. However, as EP_2 happens at the incidence near the laser mode, leading to a large value of $|\partial r_{G(p)}/\partial\theta_i|^2\tan^2\theta_i$ [see Fig. 4(g)], the transverse displacement of δ^H near EP_2 is restricted into a tiny value, as shown in Fig. 4(f). Similarly, the enhanced transverse displacement of δ^V is achieved near the resonant angle of the laser mode from p-polarization [see Fig. 4(h)], and the maximum transverse displacement can reach 4.5λ. It is obvious that the sign change of the enhanced transverse displacements of reflected light is also found at these EPs and the laser mode, which is also induced by the phase change of π at EPs and the laser mode [29]. By comparing the transverse displacements in Fig. 4, as EPs not only happen in p-polarization but also in s-polarization, the enhanced SHE of reflected light in the PT symmetric system could function not only for H-polarized incident beam but also for V-polarized incident beam, which breaks through the polarization limit in common media. By exciting the laser mode, the enhanced SHE of reflected light can occur independent of incident directions. In particular for the incidence near EPs (e.g., $\theta_i = 8.02°$ near EP_1), large spin splitting with transverse displacement of about 1.68λ occurs for the incidence from the loss side; while tiny spin splitting with transverse displacement of about 0.035λ happens for the incidence from the gain side. The contrast ratio of the transverse displacements in opposite incident directions is about 48. Therefore, asymmetric SHE featured by incident direction could be achieved through unidirectional reflectionlessness, which is different from the asymmetric SHE featured by the handedness of incident polarization [31].

5 Discussion and conclusion

In conclusion, by introducing more extraordinary PT effects, our work provided more complete picture of new behavior of SHE in PT symmetric systems, including both transmitted light beam and reflected light beam. We find that the intensive transmission induced by the laser mode in PT symmetric system can bring about the enhanced transverse displacement of transmitted light beam, therefore providing a feasible way to obtain enhanced SHE of transmitted light. In addition, the enhanced transverse displacement of reflected light could be obtained near the laser mode, regardless of the incidence from the loss or gain side. Although multiple EPs occur in the PT symmetric bilayer, the enhanced SHE of reflected light only happens near the EPs away from the laser mode. Therefore, SHE of reflected light via EPs could not be enhanced in some certain cases [32]. As EPs can lead to unidirectional reflectionlessness, asymmetric SHE (incidence-dependent spin splitting) is achieved near EPs. Considering recent advances in non-Hermitian optics, in particular for unidirectional reflectionlessness in non-ideal PT systems [24, 33] and the CPA-laser mode in PT symmetric periodic structures [34, 35], our proposed scheme to access enhanced SHE is promising and therefore enables more possibilities in manipulating photonic SHE, which might lead to more exploration of photonic SHE in non-Hermitian systems, such as conjugate metamaterials [36–40].

Acknowledgements This work was supported by the National Natural Science Foundation of China (Grant Nos. 11904169 and

61675095) and the Natural Science Foundation of Jiangsu Province (Grant No. BK20190383).

References and notes

1. M. Onoda, S. Murakami, and N. Nagaosa, Hall effect of light, *Phys. Rev. Lett.* 93(8), 083901 (2004)
2. O. Hosten and P. Kwiat, Observation of the spin Hall effect of light via weak measurements, *Science* 319(5864), 787 (2008)
3. Y. Qin, Y. Li, H. Y. He, and Q. H. Gong, Measurement of spin Hall effect of reflected light, *Opt. Lett.* 34(17), 2551 (2009)
4. X. Zhou, X. Ling, Z. Zhang, H. Luo, and S. Wen, Observation of spin Hall effect in photon tunneling via weak measurements, *Sci. Rep.* 4(1), 7388 (2015)
5. O. Takayama and G. Puentes, Enhanced spin Hall effect of light by transmission in a polymer, *Opt. Lett.* 43(6), 1343 (2018)
6. K. Y. Bliokh and A. Aiello, Goos–Hänchen and Imbert–Fedorov beam shifts: An overview, *J. Opt.* 15(1), 014001 (2013)
7. H. Luo, X. Zhou, W. Shu, S. Wen, and D. Fan, Enhanced and switchable spin Hall effect of light near the Brewster angle on reflection, *Phys. Rev. A* 84(4), 043806 (2011)
8. L. Kong, X. Wang, S. Li, Y. Li, J. Chen, B. Gu, and H. Wang, Spin Hall effect of reflected light from an air-glass interface around the Brewster's angle, *Appl. Phys. Lett.* 100(7), 071109 (2012)
9. M. Pan, Y. Li, J. Ren, B. Wang, Y. Xiao, H. Yang, and Q. Gong, Impact of in-plane spread of wave vectors on spin Hall effect of light around Brewster's angle, *Appl. Phys. Lett.* 103(7), 071106 (2013)
10. Y. Xu, Y. Fu, and H. Chen, Planar gradient metamaterials, *Nat. Rev. Mater.* 1(12), 16067 (2016)
11. T. Tang, C. Li, and L. Luo, Enhanced spin Hall effect of tunneling light in hyperbolic metamaterial waveguide, *Sci. Rep.* 6(1), 30762 (2016)
12. O. Takayama, J. Sukham, R. Malureanu, A. V. Lavrinenko, and G. Puentes, Photonic spin Hall effect in hyperbolic metamaterials at visible wavelengths, *Opt. Lett.* 43(19), 4602 (2018)
13. H. Wang and X. Zhang, Unusual spin Hall effect of a light beam in chiral metamaterials, *Phys. Rev. A* 83(5), 053820 (2011)
14. X. Yin, Z. Ye, J. Rho, Y. Wang, and X. Zhang, Photonic spin Hall effect at metasurfaces, *Science* 339(6126), 1405 (2013)
15. Y. Fu, L. Xu, Z. Hang, and H. Chen, Unidirectional transmission using array of zero-refractive-index metamaterials, *Appl. Phys. Lett.* 104(19), 193509 (2014)
16. Y. Fu, Y. Xu, and H. Chen, Additional modes in a waveguide system of zero-index-metamaterials with defects, *Sci. Rep.* 4(1), 6428 (2015)
17. Y. Fu, Y. Xu, and H. Chen, Inhomogeneous field in cavities of zero index metamaterials, *Sci. Rep.* 5(1), 11217 (2015)
18. W. Zhu and W. She, Enhanced spin Hall effect of transmitted light through a thin epsilon-near-zero slab, *Opt. Lett.* 40(13), 2961 (2015)
19. T. Tang, J. Li, L. Luo, P. Sun, and Y. Zhang, Loss enhanced spin Hall effect of transmitted light through anisotropic epsilon-and mu-near-zero metamaterial slab, *Opt. Express* 25(3), 2347 (2017)
20. T. Tang, J. Li, Y. Zhang, C. Li, and L. Luo, Spin Hall effect of transmitted light in a three-layer waveguide with lossy epsilon-near-zero metamaterial, *Opt. Express* 24(24), 28113 (2016)
21. W. Zhu, J. Yu, H. Guan, H. Lu, J. Tang, Y. Luo, and Z. Chen, Large spatial and angular spin splitting in a thin anisotropic e-near-zero metamaterial, *Opt. Express* 25(5), 5196 (2017)
22. L. Feng, R. El-Ganainy, and L. Ge, Non-Hermitian photonics based on parity–time symmetry, *Nat. Photonics* 11(12), 752 (2017)
23. Z. Lin, H. Ramezani, T. Eichelkraut, T. Kottos, H. Cao, and D. N. Christodoulides, Unidirectional invisibility induced by PT-symmetric periodic structures, *Phys. Rev. Lett.* 106(21), 213901 (2011)
24. L. Feng, Y. L. Xu, W. S. Fegadolli, M. H. Lu, J. E. B. Oliveira, V. R. Almeida, Y. F. Chen, and A. Scherer, Experimental demonstration of a unidirectional reflectionless parity–time metamaterial at optical frequencies, *Nat. Mater.* 12(2), 108 (2013)
25. S. Longhi, PT-symmetric laser absorber, *Phys. Rev. A* 82(3), 031801 (2010)
26. Y. D. Chong, L. Ge, and A. D. Stone, PT-symmetry breaking and laser-absorber modes in optical scattering systems, *Phys. Rev. Lett.* 106(9), 093902 (2011)
27. M. Tang, X. Zhou, H. Luo, and S. Wen, Spin Hall effect of a light beam in anisotropic metamaterials, *Chin. Phys. B* 21(12), 124201 (2012)
28. Y. Cao, Y. Fu, Q. Zhou, Y. Xu, L. Gao, and H. Chen, Giant Goos-Hänchen shift induced by bounded states in optical PT-symmetric bilayer structures, *Opt. Express* 27(6), 7857 (2019)
29. Y. Fu, Y. Xu, and H. Chen, Zero index metamaterials with PT symmetry in a waveguide system, *Opt. Express* 24(2), 1648 (2016)
30. Y. Fu, X. Zhang, Y. Xu, and H. Chen, Design of zero index metamaterials with PT symmetry using epsilon-near-zero media with defects, *J. Appl. Phys.* 121(9), 094503 (2017)
31. X. Zhou and X. Ling, Unveiling the photonic spin Hall effect with asymmetric spin-dependent splitting, *Opt. Express* 24(3), 3025 (2016)
32. X. Zhou, X. Lin, Z. Xiao, T. Low, A. Alù, B. Zhang, and H. Sun, Controlling photonic spin Hall effect via exceptional points, *Phys. Rev. B* 100(1), 013813 (2019)

33. R. Bai, C. Zhang, X. Gu, X. Jin, Y. Zhao, and Y. Lee, Switching the unidirectional reflectionlessness by polarization in non-ideal PT metamaterial based on the phase coupling, *Sci. Rep.* 7(1), 10742 (2017)
34. Z. Wong, Y. Xu, J. Kim, K. O'Brien, Y. Wang, L. Feng, and X. Zhang, Lasing and anti-lasing in a single cavity, *Nat. Photonics* 10(12), 796 (2016)
35. L. Ge and L. Feng, Contrasting eigenvalue and singular-value spectra for lasing and antilasing in a PT-symmetric periodic structure, *Phys. Rev. A* 95(1), 013813 (2017)
36. Y. Xu, Y. Fu, and H. Chen, Electromagnetic wave propagations in conjugate metamaterials, *Opt. Express* 25(5), 4952(2017)
37. Y. Fu, Y. Cao, S. A. Cummer, Y. Xu, and H. Chen, Coherent perfect absorber and laser modes in purely imaginary metamaterials, *Phys. Rev. A* 96(4), 043838 (2017)
38. P. Bai, K. Ding, G. Wang, J. Luo, Z. Zhang, C. T. Chan, Y. Wu, and Y. Lai, Simultaneous realization of a coherent perfect absorber and laser by zero-index media with both gain and loss, *Phys. Rev. A* 94(6), 063841 (2016)
39. Y. Fu, Y. Xu, and H. Chen, Negative refraction based on purely imaginary metamaterials, *Front. Phys.* 13(4), 134206 (2018)
40. Y. Fu, Y. Xu, H. Chen, and S. A. Cummer, Coherent perfect absorption and laser modes in a cylindrical structure of conjugate metamaterials, *New J. Phys.* 20, 013015(2018)